Civil and Environmental Science Journal
Vol. 05, No. 02, pp. 171-182, 2022

Comparison of SPT and V_s-based liquefaction assessment on young volcanic sediment: a case study in Bantul District of Yogyakarta, Indonesia.

Anisa Nur Amalina [1,4], Teuku Faisal Fathani [2,4], Wahyu Wilopo [3,4]

[1] Department of Civil Engineering, Faculty of Civil Engineering and Planning, Islamic University of Indonesia, Indonesia
[2] Department of Civil and Environmental Engineering, Faculty of Engineering, Universitas Gadjah Mada, Yogyakarta, Indonesia
[3] Department of Geological Engineering, Faculty of Engineering, Universitas Gadjah Mada, Yogyakarta, Indonesia
[4] Center for Disaster Mitigation and Technological Innovation (GAMA-InaTEK) Universitas Gadjah Mada, Yogyakarta, Indonesia

corresponding author's e-mail: amalina.anisa@gmail.com

Received 01-07-2022; accepted 27-09-2022

Abstract. On May 26, 2006, an earthquake of moment magnitude (M_w) 6.3 occurred in Yogyakarta. The damages found in Bantul were predicted to be caused by liquefaction. Moreover, liquefaction symptoms were found, such as a sand boil and lateral spreading. It inferred that the damage was controlled by the amplification factors from young redeposited volcanic sediments and altered volcaniclastics from the active Mount Merapi. This study compared subsurface conditions based on two field investigation methods (SPT and Shear Wave Velocity) and determined the liquefaction potential by considering groundwater and the region's seismicity. To obtain the most fitted equation, several equations to represent the N-SPT and V_s data were also analyzed. As a result, several equations used in this study were inadequate to correlate N-SPT and V_s properly. A comparison of safety factor values indicated that the liquefaction potential in the studied area on the V_s-based method is lower than the result from the SPT-based method.

Keywords: shear wave velocity, downhole test, N-SPT value, liquefaction potential.

1. Introduction

A strike-slip earthquake happened on May 26, 2006, in Yogyakarta. Approximately 5,700 people were killed, and over 156,000 houses and other structures were destroyed. The magnitude was 6.3, and its duration was about 60 seconds, with the hypocenter at the east of the Opak River [1, 2].

Northeast of the Parangtritis, the Bantul and Klaten are the most affected area [3]. Meanwhile, heavy losses were founded near the Opak fault was due to the amplification factors from soft sediments redeposited from the active Mount Merapi [4, 1].

Besides damaging hundreds of houses, the earthquake destroyed university and school buildings, offices, infrastructures, and the runway at Adi Sutjipto International Airport. Additionally, liquefaction symptoms were detected, such as sand boils and lateral spreading. The area with the highest potential for liquefaction is Patalan, Bantul, part of the Bantul basin, or the Opak River Fault basin [5].

Evaluating soil liquefaction is crucial to minimize future damage, especially in earthquake-prone regions. The method mainly used is the Simplified Procedure [6], originally developed from the standard penetration test (SPT) and correlated with a cyclic stress ratio parameter representing the cyclic soil loading. Meanwhile, the most common approach is in-situ V_s measurements [7]. V_s is a field measurement with less than 10−4% strain [[8], [9]]. The V_s-based liquefaction analysis has obtained considerable relevance compared to SPT-based analysis. Furthermore, V_s and liquefaction resistance are sensitive to relative density, effective stress, and cementation in the same direction [10].

This study aims to compare subsurface conditions based on two field investigation methods (SPT and Shear Wave Velocity) and determine the liquefaction potential by considering groundwater and the region's seismicity. Furthermore, a comprehensive analysis of liquefaction potential on young volcanic sediment was conducted by comparing the N-SPT and V_s values.

2. Methodology

The initial stage of this study involves seismic and geotechnical data compilation from the previous research, field test, and desk study. Next, the collected data were analyzed to determine the site classification, soil stratigraphy, and soil parameters.

Groundwater and the region's seismicity were considered to calculate the potential of liquefaction. The liquefaction analyses were conducted using the SPT method [14] and V_s measurement [6, 16, 17]. Furthermore, a comprehensive analysis of N-SPT relationships with V_s on young volcanic sediment was explained further.

2.1. Geological Conditions

The study was conducted in the Bantul Region of Yogyakarta, Indonesia. Bantul is considered earthquake-prone due to its proximity to the Eurasian Plate's subduction and the Australian plate). Furthermore, based on Rahardjo et al. [11], the Bantul region consists of quaternary young Merapi volcano deposits (Qmi) that have a high potential to liquefy (Figure 1)

Deposits in the quaternary period are divided into Holocene and Pleistocene, while deposits older than the Pleistocene are included in the tertiary period. The tertiary period comprised the Kulon Progo mountains and the southern mountains. Meanwhile, most of the quaternary deposits compose Yogyakarta and Bantul.

The lithology of the young Merapi Volcano deposits can be classified based on grains size distribution, namely 1) Sand sediment, the most dominant sediment, consists of sand, silt sand, and gravel sand, 2) silt deposits, and 3) clay sediment consists of sandy clay and clay [12].

The microtremor survey was conducted in several severely damaged locations by the 2006 earthquake [13]. The result shows that the depth of bedrock in Bantul area is approximately 30–60 meters. Meanwhile, the deepest bedrock, around 60–100 meters, lay in the east Bantul. In Jetis, Imogiri, and Pundong, a breccia layer reaches 50 meters in thickness.

2.2. Site Classification

Besides soil stratigraphy, site classification was also conducted. The classification was based on the average value of N-SPT and V_s until a depth of 30 m. The site classification can be seen in Table 1.

Site classification is commonly used to define the Peak Ground Acceleration (PGA) value by determining the seismic zones. Meanwhile, this study applied the PGA value referred to Fathani et al. [17], where the research location was also conducted in Bantul. They calculated the PGA value using an attenuation relationship considering two Scenarios of epicenter coordinate and hypocenter depth based on the Indonesia Meteorological, Climatological, and Geophysical Agency (BMKG) and the United States Geological Survey (USGS). The results are summarized in Table 2.

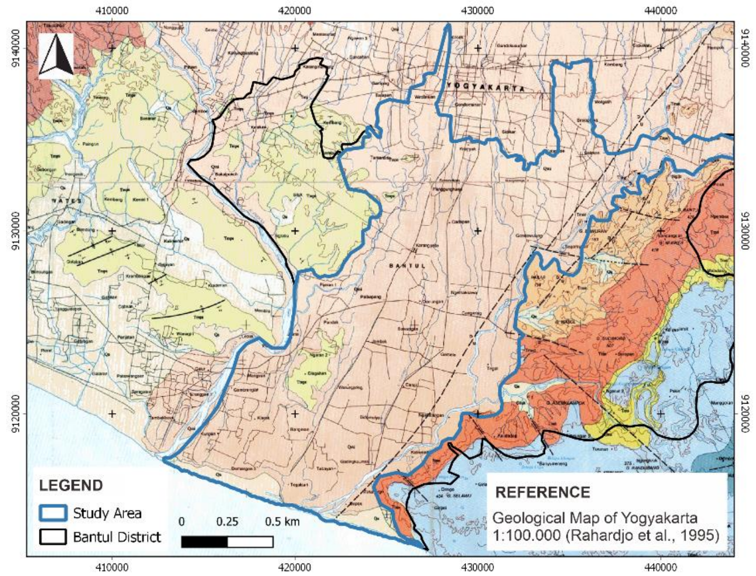

Figure 1. The location and geological condition of the study area (modified from [11]).

Table 1. Comparison of PGA based on two scenarios [17].

Site class	V_s (m/s)	$\overline{N_{30}}$
SE (soft soil)	<175	<15
SD (medium soil)	175 to 350	15 to 50
SC (hard/very dense soil and soft rock)	350 to 750	>50
SB (rock)	750 to 1500	N/A
SA (hard rock)	>1500	N/A
SF (special soil)	Required specific geotechnical investigation and site response analysis on every site	

Table 2. Comparison of PGA based on two scenarios [17].

Sample	Location	PGA (*g*)	
		BMKG	USGS
BH-01	BPKP-1	0.24	0.25
BH-02	BPKP-2	0.24	0.25
BH-03	Segoroyoso	0.25	0.30
BH-04	Karangsemut	0.26	0.30
BH-05	Wijirejo	0.28	0.24
BH-06	Bambanglipuro	0.32	0.26
BH-07	Pranti	0.30	0.30
BH-08	Tempuran Kali Opak-Oyo	0.30	0.30
BH-09	Watu	0.32	0.27

2.3. N-SPT and V_s Empirical Correlation for Young Sediment Volcanic

The data applied in this study are collected from an extensive geotechnical borehole, downhole and laboratory tests. The data consist of 29 boreholes and nine shear wave velocity data. The data depths vary from 20 m to 50 m (Figure 2). Nine borehole and downhole data were used to calculate the liquefaction potential by comparing those data. Meanwhile, the other available data were used to generate soil stratigraphy.

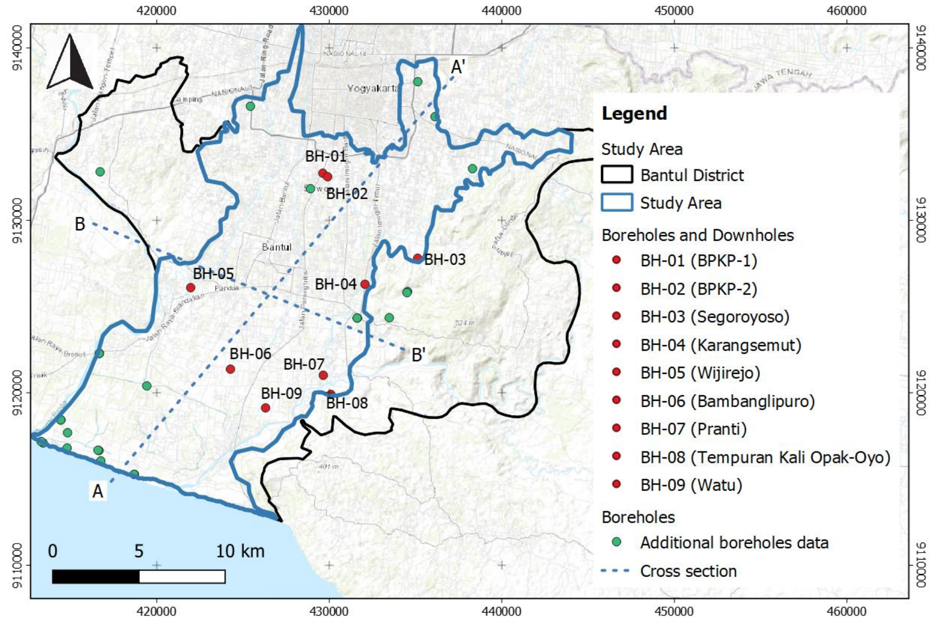

Figure 2. The location and geological condition of the study area (modified from [11]).

Several equations in Table 3 correlate the N-SPT value with shear wave velocity (V_s) in various types of soils. The selected equation was then used to define V_s value in young sediment volcanic.

Table 3. Comparison of PGA based on two scenarios [17].

Author	Equation	
Seed and Idriss [6]:	$V_s = 61.4(N)^{0.5}$	(1)
Hasancebi and Ulusay [19]:	$V_s = 90(N)^{0.39}$	(2)
Imai and Yoshimura [20]:	$V_s = 76(N)^{0.33}$	(3)
Kanai [21]:	$V_s = 19(N)^{0.6}$	(4)
Akin et al. [22]:	$V_s = 121.75(N)^{-0.101}(z)^{0.216}$	(5)
Alluvial sands [23]:	$V_s = 87.8(N)^{0.292}$	(6)
Alluvial soils (Korea) [23]:	$V_s = 82(N)^{0.319}$	(7)

2.4. Liquefaction Safety Factor (FS)

Parameters that need to be reviewed regarding liquefaction are the earthquake loading and soil strength against earthquake loading. The safety factor is calculated by comparing the cyclic stress ratio (CSR) and the cyclic resistance ratio (CRR). Liquefaction might happen if the CRR is less than CRR. The safety factor of the liquefaction is 1.2 [24].

Referring to Pawirodikromo et al. [25], the de-aggregation results found that the dominant magnitude and the distance were influenced mainly by the shallow crustal instead of the Megathrust earthquake source. The M_D= 6.5 and the R_D= 14.5 km. The Opak river fault is located approximately 10 km from Yogyakarta, while the megathrust earthquakes, with a larger magnitude, are located more than 300 km from Yogyakarta. Thus, the moment magnitude of 6.5 is used to calculate MSF (Eq. (8)).

$$\mathrm{MSF} = 6.9\exp\left(\frac{-M_w}{4}\right) - 0.058 \tag{8}$$

2.4.1. SPT-based Liquefaction Safety Factor (FS_L)
The safety factor is calculated by the cyclic stress ratio (CSR) and the cyclic resistance ratio ($CRR_{7.5}$), as shown in Eq. (9). The CSR value is adjusted to a specific earthquake magnitude (M_w=6.5) by a magnitude scaling factor (MSF).

$$\mathrm{FS_L} = \frac{\mathrm{CRR}_{7.5}}{\mathrm{CSR}}\mathrm{MSF} \tag{9}$$

2.4.2. V_s-based Liquefaction Safety Factors (FS_{Vs})
FS_{Vs} is calculated using equation given by *[6]*, [15], and [16]. The equation is generally considering both SPT and V_s data.

$$\mathrm{FS}_{V_s} = \frac{\mathrm{CRR}_{V_s}}{\mathrm{CSR}_{V_s}} = \frac{\mathrm{SRR}}{\mathrm{SSR}} \tag{10}$$

2.5. Cyclic Stress Ratio (CSR)
The CSR due to earthquake force is usually explained as 0.65 multiplied by the peak value of cyclic shear stress at a particular depth (z). Several parameters, such as surface acceleration and total and effective stresses at different depths, are considered in determining the CSR.

2.5.1. SPT-based Liquefaction Triggering Analysis (*CSR*)
The liquefaction triggering analysis proposed by Idriss and Boulanger [14] is based on trial and error $(N_1)_{60cs}$. The soil is unlikely to liquefy if the clean granular soils or $(N_1)_{60cs}$ value is larger than 30 blows/ft.

Seed and Idriss [6] calculated the induced stress ratio CSR as shown in Eqs. (11) to (14). σ_{av} is the 65% of the peak induced cyclic shear stress triggered by an earthquake, PGA or a_{max} is the peak ground acceleration at the site, g is the acceleration of gravity, r_d is a depth factor, σ_v is the initial total vertical stress, and σ'_{v0} is the initial vertical effective stress in the ground.

$$\mathrm{CSR} = \frac{\tau_{av}}{\sigma_v'} = 0.65\left(\frac{a_{\max}}{g}\right)\left(\frac{\sigma_v}{\sigma_v'}\right)r_d \tag{11}$$

$$\alpha(z) = \left[-1.012 – 1.126\sin\left(\frac{z}{11.73} + 5.133\right)\right] \tag{12}$$

$$\beta(z) = \left[0.106 + 0.118\sin\left(\frac{z}{11.28} + 5.1242\right)M_w\right] \tag{13}$$

$$r_d = \exp\left(\alpha(z) + \beta(z)M_w\right) \tag{14}$$

2.5.2. V_s-based Liquefaction Triggering Analysis (*SSR*)
The CSR parameter is changed into a shear stress ratio (SSR) in the V_s-based method. However, they have similar physical meanings. The shear stress ratio depends on the soil medium, unit weight, acceleration, and earthquake period [16].

Eqs. (15) to (17) show several parameters. First, t is a predominant period of the earthquake wave. For example, the dominant vibration period suggested for $M_{6.5}$ is 0.280s [15].

$$\mathrm{SSR} = \left(\frac{a_{\max}}{g}\right)\left(\frac{\sigma_{V_s}}{\sigma_{V_s}'}\right)r_d \tag{15}$$

$$\sigma_{V_s} = 0.25T\left(\sum_{i=1}^{n}\gamma_i V_{s_i}\right) \tag{16}$$

$$\sigma_{V_s}' = 0.25T\left(\sum_{i=1}^{n}\gamma_i V_{s_i} - V_{s_n}(\gamma_{sa} - \gamma_d)\right) \tag{17}$$

The a_{max} refers to the maximum horizontal ground acceleration (m/s^2), g is the gravitational acceleration (m/s^2), σ_{Vs} is the dynamic vertical stress (kN/m^2), σ'_{Vs} is the effective dynamic vertical stress at the same depths calculated by the same parameters (kN/m^2), and r_d is the stress reduction coefficient mentioned in Eqs. (12) to (14).

2.6. Cyclic Resistance Ratio (CRR)

Soil resistance or CRR is soil's capacity at a particular depth and state to resist liquefaction triggering liquefaction resistance is generally characterized by penetration resistance modified to account for various additional variables that can affect liquefaction resistance.

2.6.1. SPT-based Liquefaction Resistance Analysis (CRR)

The CSR parameter is changed into a shear stress ratio (SSR) in the V_s-based method. However, they have similar physical meanings. The shear stress ratio depends on the soil medium, unit weight, acceleration, and earthquake period [16].

The liquefaction safety factor can be calculated with widely used methods such as N-SPT data and corrected with five correction factors as given by [14]. The value of clean sand, $(N_1)_{60cs}$, is then obtained by adjusting the FC (fines content) to the corrected blow count.

The empirical procedures to obtain the corrected SPT values based on Idriss and Boulanger [14] are shown in Eqs. (18) to (21). Meanwhile, the SPT-based CRR relationships are presented in Eqs. (22) to (25).

$$\left(N_1\right)_{60} = N_{60} C_N C_E C_B C_R C_S \tag{18}$$

$$\mathrm{C_N} = \left(\frac{P_a}{\sigma_v'}\right)^{0.784-0.0768\sqrt{(N_1)_{60}}} \leq 1.7 \tag{19}$$

$$\Delta\left(N_1\right)_{60} = \exp\left(1.63 + \frac{9.7}{\mathrm{FC}+0.01} - \left(\frac{15.7}{\mathrm{FC}+0.01}\right)^2\right) \tag{20}$$

$$\left(N_1\right)_{60cs} = \left(N_1\right)_{60} + \Delta\left(N_1\right)_{60} \tag{21}$$

$$\mathrm{CRR}_{\sigma'=1atm} = \exp\left\{\left[\frac{(N_1)_{60cs}}{14.1}\right] + \left[\frac{(N_1)_{60cs}}{126}\right]^2 - \left[\frac{(N_1)_{60cs}}{23.6}\right]^3 + \left[\frac{(N_1)_{60cs}}{25.4}\right]^4 - 2.8\right\} \tag{22}$$

$$\mathrm{CRR}_{\sigma'} = \mathrm{CRR}_{\sigma'=1atm} K_\sigma \tag{23}$$

$$K_\sigma = \min\left\{\begin{matrix} 1 - C_\sigma \ln\left(\dfrac{\sigma_{vo}'}{p_a}\right) \\ 1.0 \end{matrix}\right\} \tag{24}$$

$$C_\sigma = \frac{1}{18.9 - 2.55\sqrt{(N_1)_{60cs}}} \tag{25}$$

2.6.2. V_s-based Liquefaction Triggering Analysis (SSR)

The shear wave velocity was formulated from more than 50 sites measurement as shear resistance ratio (SRR) and determined by corrected V_s and maximum V_s ($V_{s,\,max}$) value, as shown in Eq. (26) [26]. For values of corrected shear waves in the range of 190 to 220 m/s, the curve turns upward sharply where minor changes in V_{s1} correspond to significant changes in CRR. The correlation between CRR and V_s of uncemented Holocene-age soils shows in Figure 3 [7].

$$\mathrm{SRR} = \left[a\left(\frac{V_{S_c}}{100}\right)^2 + b\left(\frac{1}{V_{S_{max}} - V_{S_c}} - \frac{1}{V_{S_{max}}}\right)\right]\mathrm{MSF} \tag{26}$$

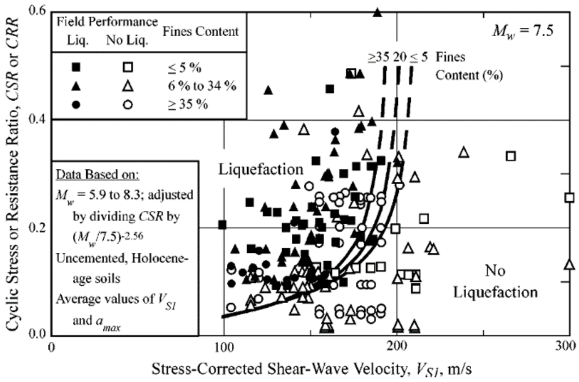

Figure 3. Correlation between CRR/CSR and V_s [7].

Uyanık and Taktak [15] determined that $V_{s\text{-max}}$ ranges from 220 to 250 m/s based on the fines content. Meanwhile, the *a* and *b* values are 0.022 and 2.8. Several researchers [27] suggested the corrected V_s formula as shown in Eqs. (27) to (28). The reference stress or atmospheric pressure (P_a) is 100 kN/m^2.

$$\begin{aligned} V_{S_{max}} &= 250 \text{ m/s, FC} \le 5\% \\ V_{S_{max}} &= 250 - (\text{FC} - 5) \text{ m/s, } 5\% < \text{FC} < 35\% \\ V_{S_{max}} &= 220 \text{ m/s, FC} \ge 35\% \end{aligned} \tag{27}$$

$$V_{S_c} = V_S\left(\frac{P_a}{\sigma_v'}\right)^{0.25} \tag{28}$$

3. Result and Discussion

3.1. Soil Classification

Soil classification was conducted by calculating the average value of N-SPT and V_s. Data less than 30 m were approached by the nearest borehole N-SPT values. Table 4 shows a summary of site classification according to [18].

The results show that all soils are considered medium soils. In contrast, several locations (BH-03, BH-04, BH-08, and BH-09) are considered soft soil from the V_s-based calculation. Consequently, this difference will affect the results of the FS calculation. In addition, it might occur due to the uncertainties in downhole field performance.

Table 4. Site classification based on SPT and V_s.

Sample	Location	Depth (m)	Soil classification	
			SPT	V_s
BH-01	BPKP-1	30	SD	SD
BH-02	BPKP-2	20	SD	SD
BH-03	Segoroyoso	46	SD	SE
BH-04	Karang-semut	20	SD	SE
BH-05	Wijirejo	46	SD	SD
BH-06	Bambang-lipuro	50	SD	SD
BH-07	Pranti	40	SD	SD
BH-08	Kali Opak-Oyo	30	SD	SE

BH-09	Watu	34	SD	SE
Notes: SD = medium soil; SE = soft soil				

3.2. Borehole Stratigraphy

A total of 23 data were analyzed to interpret the soil stratigraphy. The bedrock depth was estimated from the previous research by Perdhana and Nurcahya [13]. The soil layers are divided into fine sand, medium to coarse sand, silt to clay, breccia, medium to fine sandstone, and bedrock. The A-A' cross-section is made as long sections from north to south while the B-B' is cross-sections from west to east (Figure 2).

The borehole data show that fine sand, classified as the lithology of the Young Merapi Volcano Deposits, dominates the upper layer up to 20 m depth. Beneath the 20 m, the soil layer is composed of fine to medium sandstone layers.

Figure 4 and Figure 5 present an interpretation of the soil layer. This interpretation is coherent with the research of Buana and Agung [12], where fine sand dominates the area around the east of Bantul. In addition, in the Watu area, Imogiri and Karangsemut consist of a breccia layer.

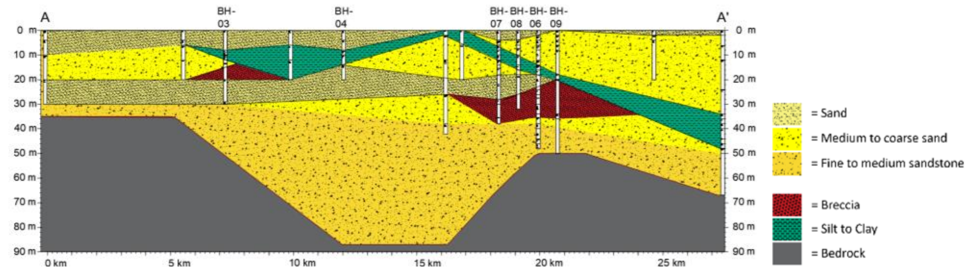

Figure 4. Soil stratigraphy of cross-section A-A′.

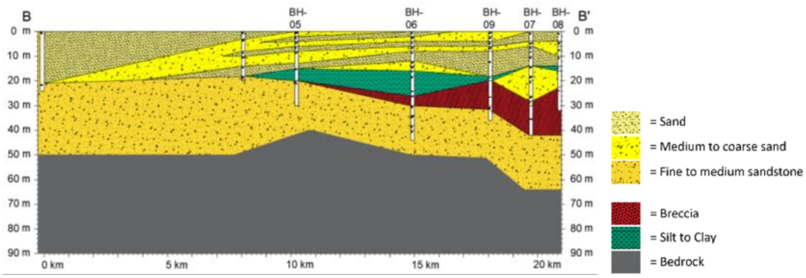

Figure 5. Soil stratigraphy of cross-section B-B′.

3.3. N-SPT and V_s correlation

Table 5 shows that the given equations cannot adequately represent the N-SPT and V_s correlation. Generally, the equation by Akin et al. [22] gives the most insignificant error compared to the other equations. In addition, the error value of BH-04 tends to be small by applying the equation intended for alluvial sediments.

Table 5. Summary of relative error for each equation.

Location	Relative Error, E_r (%)						
	Eq. 1	Eq. 2	Eq. 3	Eq. 4	Eq. 5	Eq. 6	Eq. 7
BH-01	120	75	58	58	23	62	65
BH-02	166	108	88	56	21	92	96
BH-03	148	88	71	58	30	73	78
BH-04	78	36	37	47	47	34	34
BH-05	232	149	108	161	34	107	115
BH-06	277	182	156	66	67	159	166

Location	Relative Error, E_r (%)						
	Eq. 1	Eq. 2	Eq. 3	Eq. 4	Eq. 5	Eq. 6	Eq. 7
BH-07	209	188	136	217	50	145	147
BH-08	134	96	62	111	35	65	68
BH-09	175	115	79	127	27	79	85

The previously published research mainly used statistical relation to represent V_s and N_{60} without considering confining stress. As a result, the graphs (Figure 6) show significant errors in the equations that neglect confining stress (z). Meanwhile, the other equations tend to be overestimated compared to the field test. Hence, the effects of confining stress should be considered to minimize bias and reduce uncertainty.

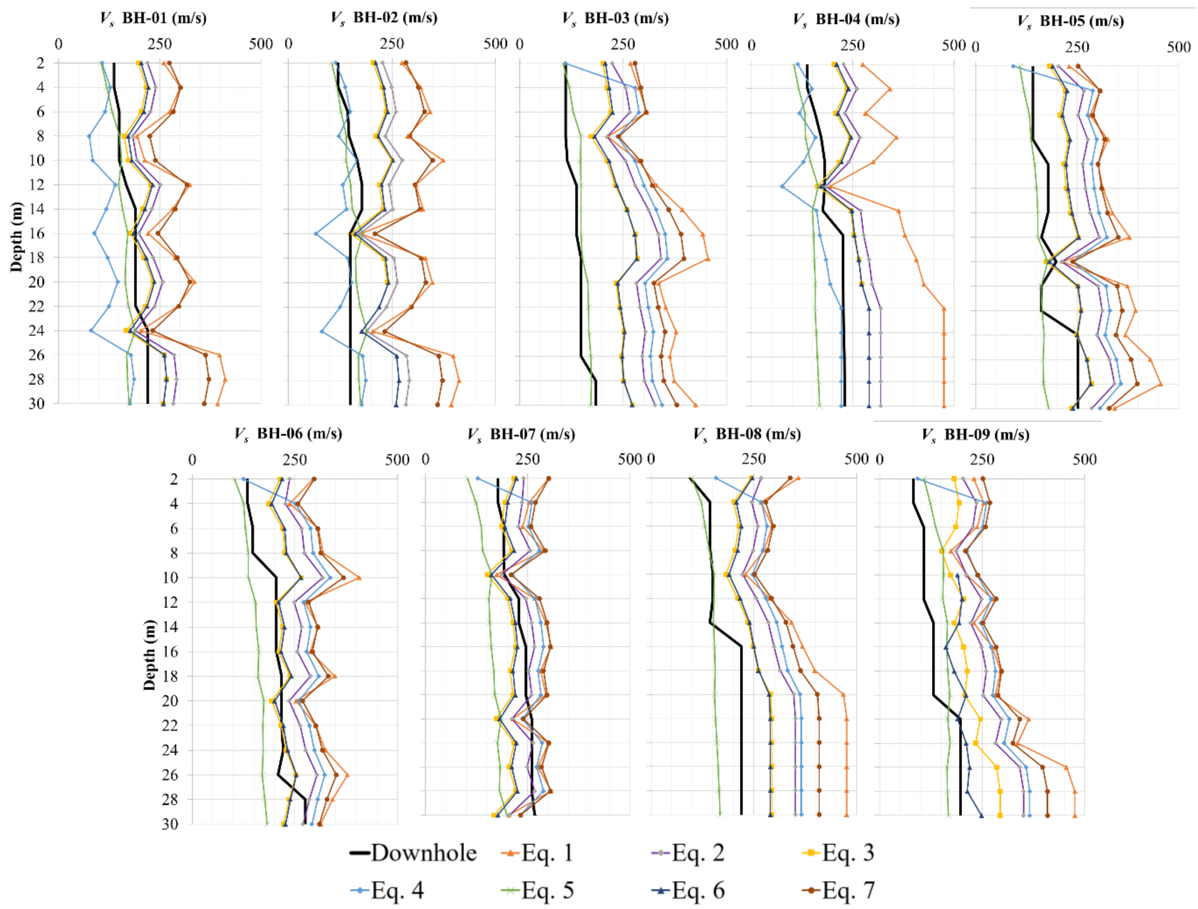

Figure 6. N-SPT and V_s correlation based on given equations.

3.4. Liquefaction analyses

The liquefaction analysis was carried out based on two methods (N-SPT and V_s-based) by considering the largest acceleration value taken from Fathani et al. [17]. Figure 7 presents the analysis result from those methods.

V_s-based results tend to be much lower than the SPT-based method. The site classification has identified this condition, where some boreholes are classified as soft soil instead of medium soil.

The formula given by Idris et al. [14] is susceptible to $(N_{30})_{cs}$ and FC values, where a value greater than 30 might result in an FS value greater than 2. In contrast, the V_s-based results cannot identify these conditions. Therefore, it aligns with Ghazi et al. [27], where the V_s values decrease mainly caused by the void ratio, while the grain size distribution and relative density do not affect them.

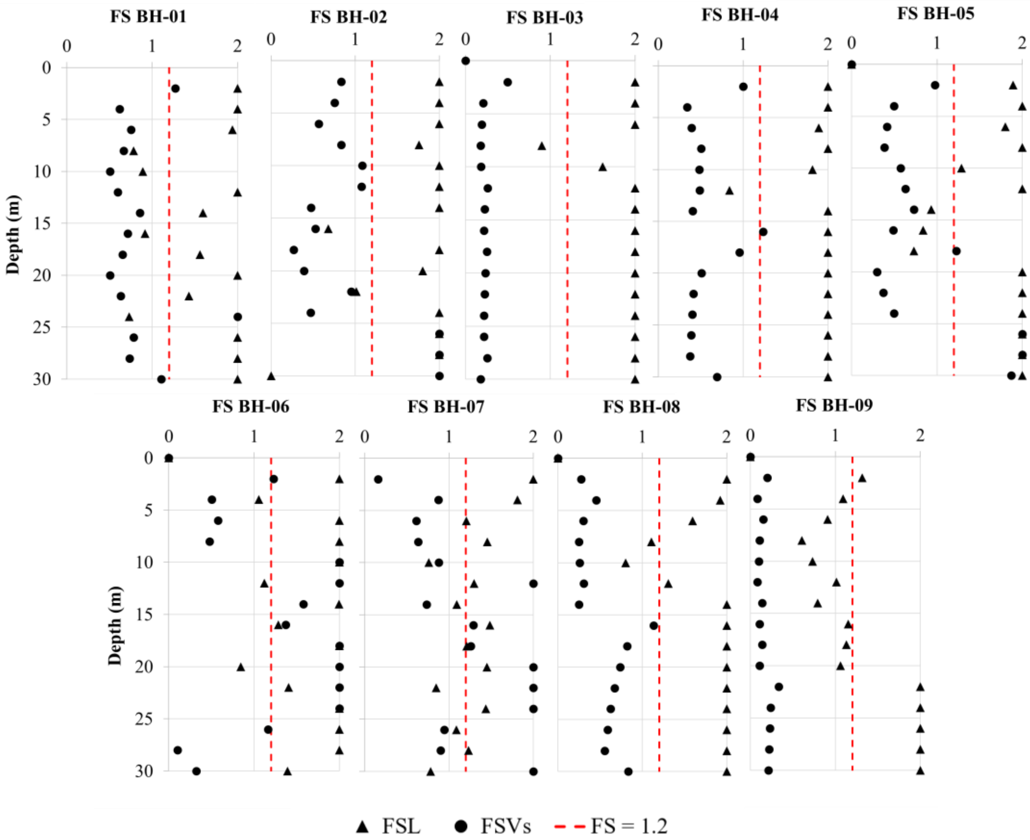

Figure 7. FS comparison based on two methods.

4. Conclusions

The present study intended to compare the liquefaction potential from SPT and V_s tests. Those methods provide slightly different results.

Indonesian code of SNI 8460:2017 [18] was used to determine the soil classification. Several locations showed different results, such as on BH-03, BH-04, BH-08, and BH-09. Based on SPT data, the soil is classified as medium sand, while in V_s -based, it is classified as soft soil.

Several equations in this study are inadequate to deliver a good correlation between N-SPT and V_s. The error value varies between 30 - 200%. However, the equation by Akin et al. [22] gave the smallest error number. Therefore, additional borehole and downhole tests must be carried out in the study area to determine the most compatible equation for the Young Volcanic Sediment.

The comparison of the safety factor values indicated that the liquefaction potential in the studied area on the V_s-based method is lower than the result from the SPT-based method. Such differences may occur due to the errors and uncertainties in both borehole and downhole field performance.

References

[1] USGS Preliminary Earthquake Report, The website of United StatesGeological Survey, Earthquake Hazards Program, (available athttp://earthquake.usgs.gov/eqcenter/eqinthenews /2006/usneb6/), 2006.

[2] A.S. Enashai, S.J. Kim, G.J. Yun, and D. Sidarta, *The Yogyakarta Earthquake of May 27 2006*. Mid-American Earthq. Center, Un. of Illinois at Urbana Champaign, 2006.

[3] H.Z. Abidin, H. Andreas, T. Kato, T. Ito, I. Meilano, F. Kimata, D.H. Natawidjaya, and H. Harjono, "Crustal deformation studies in Java (Indonesia) using GPS," *J. Earthq. Tsunami*, vol. 3, pp. 77–88, 2009.

[4] T.R. Walter, R. Wang, M. Zimmer, H. Grosser, B. Luhr, and A. Ratdomopurbo, *Volcanic activity influenced by tectonic earthquakes-Static and dynamic stress triggering at Mount Merapi*. Geophysical Research Letters, 34. 2007.

[5] E. Soebowo, A. Tohari, and D. Sarah, "Liquefaction Potential Due to Earthquake Based on CPT and N-SPT Data in Patalan Region Bantul, Yogyakarta," *J. Geol. and Min. Resc*, vol. 19, no. 2, pp. 85-97, 2009.

[6] H.B. Seed and I.M. Idriss, "Simplified procedure for evaluating 255 soil liquefaction potential." *J. Soil Mech. Found. Div.*, vol. 97, pp. 1249–1273, 1971.

[7] R. D. Andrus and K. H. Stokoe, "Liquefaction Resistance of Soils from Shear-Wave Velocity," *J. Geo. Geoenv. Eng.*, vol. 126, no. November, pp. 1015–1025. 2000.

[8] R. D. Andrus, K. H. Stokoe, and C.H Juang, "Guide for Shear-Wave Based Liquefaction Potential Evaluation," *Earth. Spec.*, vol. 20, pp. 285–308, 2004.

[9] El-Sekelly, T. Abdoun, R. Dobry, "Centrifuge Modeling of the Effect of Preshaking on the Liquefaction Resistance of Silty Sand Deposits," *J. Geo. Geoenv. Eng.*, vol. 142(6):04016012, 2016.

[10] K. Tokimatsu and A. Uchida, "Correlation between liquefaction resistance and shear wave velocity," *Soils Found.,* vol. 30 (2), pp. 33–42, 1990

[11] W. Rahardjo, Sukandarrumidi, and H.M.D. Rosidi, *Geological map of Yogyakarta sheet Jawa*. (Bandung: Geological Research and Development Centre), 1995.

[12] T.W. Buana and M.W. Agung, "Liquefaction Characteristic Based on Ground Response Linier Equivalent Analysis and Cyclic Stress Concept on Young Merapi Volcanic Deposit in Bantul," *J. Jap. Soc.Eng. Geo.*, pp. 1–5, 2015.

[13] P. Radhitya and B. Nurcahya, "Seismic microzonation based on microseismic data and damage distribution of 2006 Yogyakarta Earthquake," *E3S Web of Conferences*. 76. 03008, 2019.

[14] I. M. Idriss and R. W. Boulanger, *Soil liquefaction during earthquakes*. Earthquake Engineering Research Institute. CA, 2008.

[15] O. Uyanik and A.G. Taktak, A New Method for Liquefaction Analysis from Shear Wave Velocity and Active Vibration Period. SDU, Science and Technology. Ins. magazine 13 (1), 74–81, 2009.

[16] O. Uyanik, B. Ekinci, and N.A. Uyanik. "Liquefaction analysis from seismic velocities and determination of lagoon limits Kumluca/Antalya example," *J. App. Geo.*, vol. 95, pp. 90–103, 2013

[17] T.F. Fathani, A.D. Adi, S. Pramumijoyo, and D. Karnawati. "The Determination of Peak Ground Acceleration at Bantul Regency, Yogyakarta Province, Indonesia," *The Yogyakarta Earthquake May 27, 2006*, pp. 1–15, 2008.

[18] Ministry of Public Works Republic of Indonesia, *National Standard of Seismic Design for Building Structure* (*SNI 8460:2017*), (Jakarta: Indonesian National Standard). 2017.

[19] N. Hasancebi and R. Ulusay, "Empirical Correlations Between Shear Wave Velocity and Penetration Resistance for Ground Shaking Assessments," *Bulletin of Engineering Geology and the Environment*, vol. 66, pp. 203–213, 2006.

[20] T. Imai and M. Yoshimura, "The Relation of Mechanical Properties of Soils to P- and S-Waves Velocities for Soil in Japan," Urana Research Institute, OYO Corporation, Tokyo, 1976.

[21] K. Kanai, "Semi-Empirical Formula for the Seismic Characteristics of the Ground Motion," Bulletin of the Earthquake Research Institute, Vol. 35, No. 2, 1957, pp. 309-325.

[22] M.K. Akin, S. Kramer, and T. Topal, "Empirical Correlations of Shear Wave Velocity (V_s) and pene- tration resistance (SPT-N) for different soils in an earthquake-prone area (Erbba-Turkey)," *J. Eng Geology*, vol. 119, pp. 1-17, 2011.

[23] W. A. Prakoso, A. Rahayu, I.A. Sadisun, A.S. Muntohar, M. Muzli, dan A. Rudyanto, "Comparing Shear-wave Velocity Determined by MASW with Borehole Measurement at Merapi Sediment in Yogyakarta," *Int. J. Technol.*, vol. 6, pp. 993–1000, 2017

[24] H. Sonmez, "Modification of The Liquefaction Potential Index and Liquefaction Susceptibility Mapping for A Liquefaction-Prone Area (Inegol, Turkey)". J. Env. Geo., vol. 44(7), pp. 862–871, 2003.

[25] W. Pawirodikromo, L. Makrup, M. Teguh, dan B. Suryo, "Development of synthetic ground motion at a specific site in Yogyakarta town, Indonesia utilizing the PSHA Method," *E3S Web of Conferences*, vol. 156, 2020.

[26] R.D. Andrus, K.H. Stokoe, "Liquefaction Resistance Based on Shear Wave Velocity in Evaluation of Liquefaction Resistance of Soils, In: T.L. Youd and I.M. Idriss (eds.)," *NCEER Proc.*, Salt Lake, UT, pp. 89-128, 1997.

[27] O. Uyanık, "An Alternative to the Repetitive Strain Ratio of Liquefied or Non-Liquified Soils," *DEU. Fen ve Müh. Dergisi*, vol. 8 (2), pp. 79–91, 2006.

[28] A. Ghazi, H. H. Moghadas, H. Sadeghi, M. Ghafoori, and G.R. Lashkaripour, "Spatial Variability of Shear Wave Velocity Using Geostatistical Analysis in Mashhad City, NE Iran," *Open J. Geol.*, 4, 354-363, 2014.